SYNCHRONIZATION IN NETWORKS OF CARDIAC CELLS

V.S. Petrov, O.I. Kanakov, G.V.Osipov, C.K. Chan and J.Kurths

***Abstract*— The cardiac muscle cells and tissues can be either oscillatory or excitable. We observed various oscillating regimes that take place in ensembles of virtual coupled cells of both types. They were simulated accordingly to the Luo-Rudy model of membrane voltage potential.**

Firstly, we studied dynamics of two coupled cells. By means of numerical simulation we have found the range of coupling parameter where the synchronous regime exists. Secondly, we considered a chain consisted of excitable cells forced by a single oscillatory cell. On the basis of the first results we have investigated the conditions of spread of oscillations from the oscillatory cell into the excitable region. After that we modified the chain by addition of one more oscillatory cell. During studies of that structure we have found different regimes of oscillating behavior such as cluster synchronization or interaction through the excitable region.

Finally, global and cluster synchronization regimes were studied in the lattice of coupled cells. Several available experimental results (formation of target and spiral waves in the cardiac cultures) were also reproduced in modeling.

I. INTRODUCTION

Cardiac cells and tissues according to their dynamics may be of two types: oscillatory cells and excitable cells. If values of various ionic conductances are set constant that difference in cells behavior is completely defined by the constant external current that flows through the membrane. When this value is increased above a bifurcation value approximate equal to -2.21 at the chosen values of parameters, a limit cycle appears in the phase space of the model, thus the cell becomes oscillatory [1]. Variation of values of certain parameters (such as ionic currents conductances, temperature etc.) causes different oscillating regimes in muscle cells. Influence of some parameters on the cell dynamics was considered with a help of numerical modeling of virtual cell.

The main issue to observe was interaction of oscillatory and excitable cells. Particularly we investigated regimes that take place in chains of such oscillators. Variety of that regimes depends on the ratio of oscillatory cells and excitable cells in the chain, the value of electric coupling coefficient, the ratio of oscillatory cells natural frequency. Beforehand we had studied the interaction of only two membranes (oscillatory cell-oscillatory cell, oscillatory cell-excitable cell) aiming at investigating of the peculiarities of that regimes for they may effect on the dynamics of the whole chain.

This work is done at financial support RFBR-NSC, project 05-02-90567 and RFBR-MF project 05-02-19815 and RFBR project 06-02-16596. G.O. and J.K. acknowledges support of EU-Network BioSim, Contract No. LSHB-CT-2004-005137

V.S.Petrov, O.I.Kanakov and G.V.Osipov are with Radiophysical department, University of Nizhny Novgorod, Gagarin ave. 23, 603950 Nizhny Novgorod, Russia; Valentin.S.Petrov@gmail.com, osipov@rf.unn.ru

C.K. Chan is with Institute of Physics, Academia Sinica, 128 Sec.2,Academia Rd., Nankang, Taipei 115, Taiwan;

J.Kurths is with Institute of Physics, University Potsdam, 10, Am Neuen Palais, D-14415, Potsdam, Germany; juergen@agnld.uni-potsdam.de

II. MODEL

The general approach is based on a numerical reconstruction of the ventricular action potential by using Hodgkin-Huxley-type formalism [2]. The rate of change of membrane potential V is given by

$$dV/dt = -(1/C)(I_i + I_{ext})$$

where C is the membrane capacitance, I_{ext} is a stimulus current, and I_i is the sum of six ionic currents: I_{Na}, a fast sodium current; I_{si}, a slow inward current; I_K, a time-dependent potassium current; I_{K1}, a time-independent potassium current; I_{Kp}, a plateau potassium current; and l_b, a time-independent background current. The ionic currents are determined by ionic gates, whose gating variables are obtained as a solution to a coupled system of eight nonlinear ordinary differential equations. The ionic currents, in turn, change V, which subsequently affects the ionic gates and currents. The differential equations are of the form

$$dy/dt = (y_\infty - y)/\tau_y$$

where

$$\tau_y = 1/(\alpha_y + \beta_y)$$

and

$$y_\infty = \alpha_y/(\alpha_y + \beta_y)$$

y represents any gating variable, τ_y is its time constant, and y_∞ is the steady-state value of y. (α_y and β_y are voltage-dependent rate constants [3]).

III. DYNAMICS OF TWO COUPLED CARDIAC CELLS

A. Interaction of two oscillatory cells

Studding this question we observed two cells which were different only in the values of external currents and in the initial conditions. The values of external currents were set to make both cells to generate oscillations. The former cell had $I_{ext} = -2.8$, and the latter had $I_{ext} = -2.2$. Using described above model we obtained the curve of dependence between cell oscillation frequency and the value of the diffusion coupling coefficient d. The result is shown in Fig. 1. Apart from it, in Fig. 2a) and 2b) time histories of the processes for $d = 0, d = 0.01$ respectively are shown. According to that pictures we can state that cells which initially had significantly different natural frequencies get eventually with increasing of coupling parameter into the synchronous regime. Moreover this synchronization is

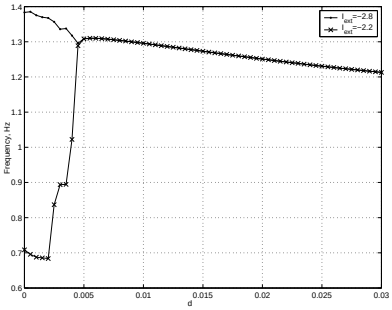

Fig. 1. Frequency of cells in dependence on coupling coeffi cient *d.*

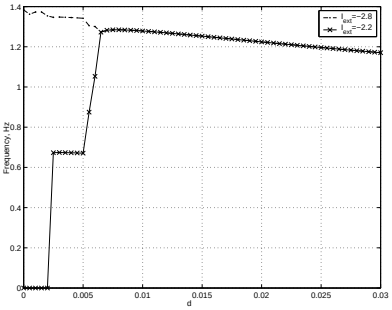

Fig. 4. Frequency of cells in dependence on coupling coeffi cient *d.*

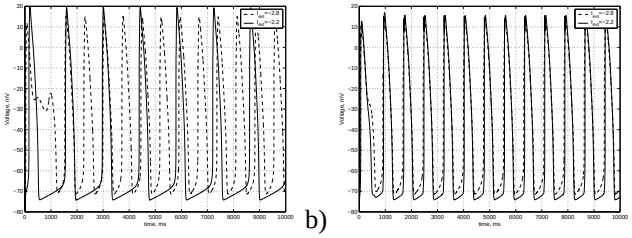

a) b)

Fig. 2. Time history of the processes for a) $d = 0$, b) $d = 0.01$.

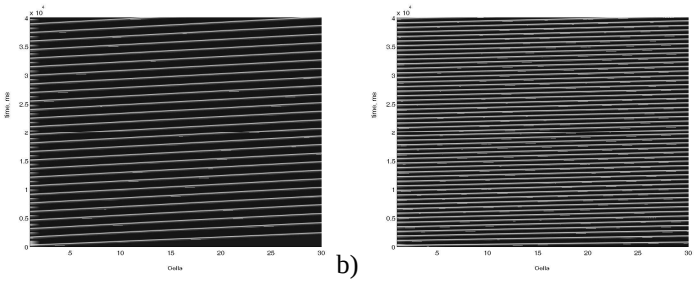

a) b)

Fig. 5. Space-time diagram for $I_{ext}^{1} = -2.8, I_{ext}^{others} = -2, d = 0.003$ (a), $d = 0.01$ (b)

inphase that we can see in the Fig. 2b). It is completely coordinated with such type of coupling as diffusion electric.

B. oscillatory cell and excitable cell interaction

At this case experiment conditions were the same as in the previous part except the value of external current of the second cell. We set for it $I_{ext} = -2$ that converts the cell into excitable regime. That fact is confirmed in Fig. 3a) where time history of process for $d = 0$ is represented. It is clearly seen that with $d = 0$ the second cell gets into the stable state $V = -72mV$. Fig. 4,3b) are analogous to the Fig. 1,2b) of the previous section. Besides, in the case of oscillatory cell and excitable cell interaction the synchronization 1:2 appears. For high values of d the inphase synchronization takes place as it was in the previous experiment.

IV. Studding cardiac cell chain dynamics

The chain we wanted to study in general had the following structure: on the right and left ends of the chain there were oscillatory cells with different natural frequencies and excitable cells between them. Elements in chain were joined through the diffusion electric coupling so that each element was joined with two its neighbors only. Exceptions were the first and the last cells of the chain. Each of them had only one coupled adjacent element.

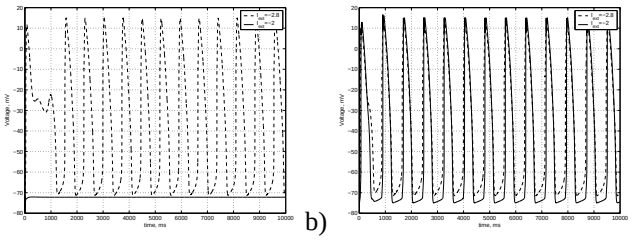

a) b)

Fig. 3. Time history of the process for a) $d = 0$, b) $d = 0.01$.

However, to study the chain described above properly, we had had to find at first the values of coupling coefficient d when oscillations of a single oscillatory cell would spread through the excitable region. To answer this question we observed a thirty-element chain. The first element was a oscillatory cell with $I_{ext} = -2.8$ and other cells were excitable with their $I_{ext} = -2$. Space-time diagrams of the oscillating processes for $d = 0.003, 0, 01$ are represented in Fig. 5a),5b) respectively. There are obviously no oscillation of excitable cells for $d = 0$. When $d = 0.003$ wave appears to spread through the excitable region, but only every second impulse of oscillatory cell propagates to the medium. That result may be easily explained on the basis of previous investigations. When we observed an interaction of one oscillatory cell and one excitable cell we saw (Fig. 4) that for $d = 0$ there was a synchronous regime 1:2. That settles it. Returning to current task we must state that with increasing of d spread of oscillations from oscillatory cell through the excitable region can be seen. And in this case regime of inphase synchronization 1:1 takes place (e.g. for $d = 0.01$ in Fig. 5b)). Thus, having studied the conditions of spread of oscillations in chain we returned to the first task. We observed thirty cells again but there were two oscillatory cells with different natural frequencies. They were the first element in chain with $I_{ext} = -2.8$ and the thirtieth element with $I_{ext} = -2.2$. Other elements had $I_{ext} = -2$ and, hence, formed the excitable structure. Fig. 6 shows the dependence between cells frequencies and coupling coefficient *d.* We can see, that in the area of small d excitable cells do not oscillate

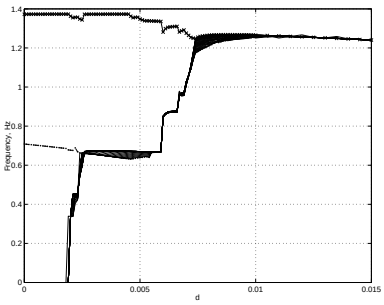

Fig. 6. Frequencies of all cells in dependence on coupling coeffi cient d. $I_{ext}^{1} = -2.8, I_{ext}^{30} = -2.2, I_{ext}^{others} = -2$.

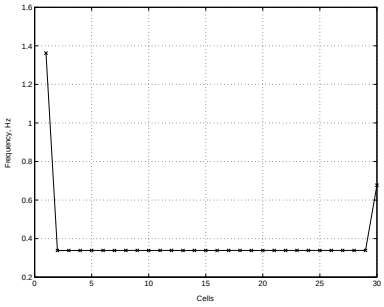

Fig. 7. Distribution of cell frequencies on elements of chain for $d = 0.002$.

meanwhile the oscillatory cells interact slightly and almost do not impact each other. With growth of d frequencies of excitable cells begin to move towards the frequency of the second oscillatory cell which has a less natural frequency than the first one. Starting from $d = 0.0056$ all excitable elements and the second oscillatory cell get into synchronous regime. Eventually they have the same frequency as the first oscillatory cell.

In addition to it we must note some remarkable points on the curve in Fig. 6. Such points are $d = 0.002, d = 0.0026$ where all excitable cells are in the synchronous regime. That situation is shown on Fig. 7. Apart from it, noticeable fact is that for range $d = 0.0055 - 0.006$ where all excitable cells and the low frequency oscillatory cell are in the synchronous regime 1:1, the high frequency oscillatory cell is also oscillating synchronously but with ratio 2:1.

Finally, for considered structure of chain an effect of cluster synchronization can be observed. Previously we saw the situations when one of oscillatory cells grasped the excitable medium (excitable cells were synchronized with one of the oscillatory cells, Fig. 6). Later we discovered that for certain parameters of our system the range of coupling coefficient d existed where some excitable cells were synchronized with one oscillatory cell and some cells were synchronized with the other one. For example, in Fig. 8 that effect is evidently represented. Here first oscillatory cell has $I_{ext} = -2.8$, second oscillatory cell has $I_{ext} = -2.7$ and coupling coefficient $d = 0.0074$.

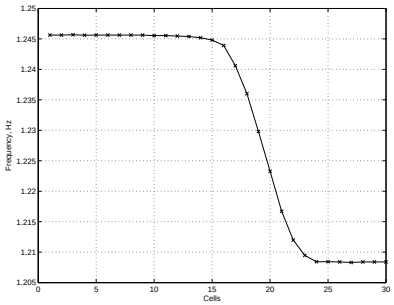

Fig. 8. Distribution of cell frequencies on elements of chain for $I_{ext}^{1} = -2.8, I_{ext}^{30} = -2.7, I_{ext}^{others} = -2, d = 0.0074$.

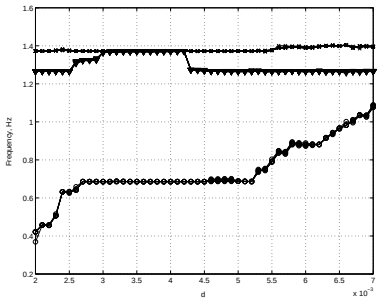

Fig. 9. Frequencies of cells in dependence on coupling coeffi cient d. $I_{ext}^{1-12} = -2.8, I_{ext}^{19-30} = -2.65, I_{ext}^{13-18} = -2$.

V. Interaction through the excitable region

In that experiment we considered a chain with modified structure. Still it was a thirty-element chain but first twelve cells were oscillatory with $I_{ext} = -2.8$, last twelve cells were also oscillatory with $I_{ext} = -2.65$ and only six excitable cells with $I_{ext} = -2$ were between them. The result of calculating frequencies of cells is shown in Fig. 9. We can see that for $d = 0.003 - 0.004$ twelve oscillatory cells which initially had less natural frequency get into synchronous regime with the other oscillatory cells. The important thing to notice is that all the excitable cells are synchronized with oscillatory cells with ratio 1:2. Distribution of frequencies on elements for $d = 0.004$ is represented in Figure 10a). Fig. 10) shows space-time diagram for this case. We also studied the dependence of that effect on size of excitable region. If the number of excitable cells between oscillatory cells increases, the range of d where synchronization of oscillatory cells

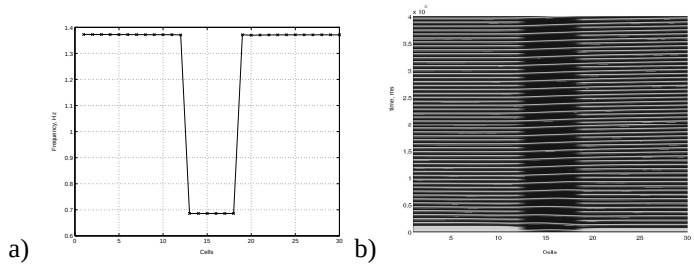

Fig. 10. a) Distribution of cell frequencies on elements of chain for $d = 0.004$. b) Space-time diagram for that case.

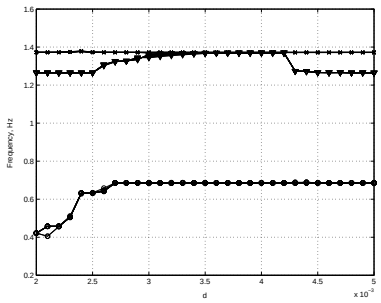

Fig. 11. Frequencies of cells in dependence on coupling coeffi cient d. $I_{ext}^{1-10} = -2.8, I_{ext}^{21-30} = -2.65, I_{ext}^{11-20} = -2$.

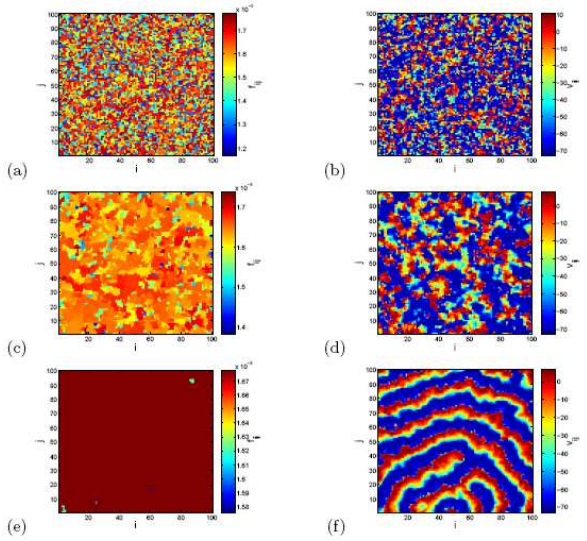

Fig. 12. Measured oscillation frequencies (a,c,e) and snapshots of membrane voltage after waiting time $8 \cdot 10^5$ units (b,d,f) in a 2D lattice of 100×100 oscillatory Luo-Rudy cells at different values of the coupling coeffi cient $d = 0.001$ (a,b), 0.002 (c,d), $d = 0.003$ (e,f).

exists will become shorter. Fig. 11 illustrates that statement. Here ten excitable cells let oscillatory cells to be synchronized for the range $d = 0.035 - 0.04$. Increasing of excitable cells number to ten caused shortening of synchronous region from 0.01 to 0.005.

VI. Two-dimensional model

We have also studied the processes of cluster synchronization and wave spread in a 2D culture of cardiac cells. Here we represent our results to make the observation of the main question more or less complete.

A square lattice of $N = M * M, M = 100$ Luo-Rudy cells were considered. The values of external current were distributed on the interval $[-2.4; -3.2]$. Fig. 12 shows the measured average oscillation frequency at 3 different values of the coupling coefficient d along with corresponding snapshots of membrane voltage v_{ij} . At small coupling $d = 0.001$ frequency clusters exist, but are no more than a few elements in size, and the activity in the lattice looks incoherent (Fig. 12 (a,b)). As coupling d increases, the clusters get larger (Fig. 12 (c,d)). After further increasing d,

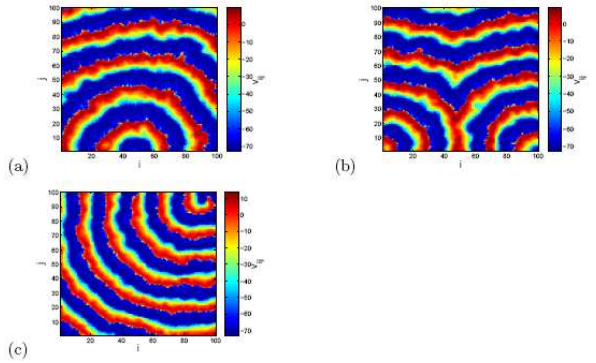

Fig. 13. Snapshots of membrane voltage after waiting time $8 \cdot 10^5$ units in a 2D lattice of 100×100 oscillatory Luo-Rudy cells for 3 different realizations of the random distribution of external currents I_{ext}^{ij} at $d = 0.004$. In all cases global synchronization up to numerical accuracy is observed.

almost the whole lattice gets covered with one cluster, except for small "defects" characterized by differing frequencies (Fig. 12 (e,f)). The corresponding space-time evolution in the latter case is an almost regular target wave structure, but it contains defects in the forms of additional oscillatory cells and spiral cores, which can coexist (Fig. 12 (f)). Such structural defects and the mentioned defects in the frequency profiles are typically well associated with each other (compare Figs. 12 (e) and (f)).

Further increasing the coupling parameter leads to a globally synchronous regime. We observe, that it can be represented as well by one oscillatory cell, two oscillatory cells and a spiral wave in different realizations of I_{ext} distribution (Fig. 13 (a,b,c), respectively) [4].

VII. Conclusions

With a help of numerical modeling was found a set of sinchronous regimes in chains and 2D lattice of cardiac cells. The effects of clustered sinchronization and interaction of oscillatory cells through the excitable region were observed.

References

[1] S. L. Lilly *Pathophysiology of Heart Disease* Lippincott Williams and Wilkins, USA, 2003.

[2] A. L. Hodgkin, A. F. Huxley *A quantitative description of membrane current and its application to conduction and excitation in nerve* J Physiol, 1952.

[3] C. H. Luo, Y. Rudy *A model of the ventricular cardiac action potential* Circ. Res., 1991.

[4] O. I. Kanakov, G. V. Osipov, C. K. Chan, J. Kurths *Cluster synchronization and spatio-temporal dynamics in networks of oscillatory and excitable Luo-Rudy cells* Chaos, 2007.